A structure–function analysis of the yeast Elg1 protein reveals the importance of PCNA unloading in genome stability maintenance

Keren Shemesh[1], Marek Sebesta[2], Martin Pacesa[2], Soumitra Sau[1], Alex Bronstein[1], Oren Parnas[1], Batia Liefshitz[1], Česlovas Venclovas[3], Lumir Krejci[2,4,5] and Martin Kupiec[1,*]

[1]Department of Molecular Microbiology and Biotechnology, Ramat Aviv 69978, Israel, [2]Department of Biology, Masaryk University, CZ-625 00 Brno, Czech Republic, [3]Institute of Biotechnology, Vilnius University, Graičiūno 8, Vilnius LT-02241, Lithuania, [4]National Center for Biomolecular Research, Masaryk University, CZ-625 00 Brno, Czech Republic and [5]International Clinical Research Center, St. Anne's University Hospital in Brno, CZ- 656 91 Brno, Czech Republic

ABSTRACT

The sliding clamp, PCNA, plays a central role in DNA replication and repair. In the moving replication fork, PCNA is present at the leading strand and at each of the Okazaki fragments that are formed on the lagging strand. PCNA enhances the processivity of the replicative polymerases and provides a landing platform for other proteins and enzymes. The loading of the clamp onto DNA is performed by the Replication Factor C (RFC) complex, whereas its unloading can be carried out by an RFC-like complex containing Elg1. Mutations in *ELG1* lead to DNA damage sensitivity and genome instability. To characterize the role of Elg1 in maintaining genomic integrity, we used homology modeling to generate a number of site-specific mutations in *ELG1* that exhibit different PCNA unloading capabilities. We show that the sensitivity to DNA damaging agents and hyper-recombination of these alleles correlate with their ability to unload PCNA from the chromatin. Our results indicate that retention of modified and unmodified PCNA on the chromatin causes genomic instability. We also show, using purified proteins, that the Elg1 complex inhibits DNA synthesis by unloading SUMOylated PCNA from the DNA. Additionally, we find that mutations in *ELG1* suppress the sensitivity of *rad5Δ* mutants to DNA damage by allowing trans-lesion synthesis to take place. Taken together, the
data indicate that the Elg1–RLC complex plays an important role in the maintenance of genomic stability by unloading PCNA from the chromatin.

INTRODUCTION

Accurate replication of the genome is essential for preserving cellular integrity. During the process of DNA replication, secondary structures and lesions may lead to the stalling of the replication fork (1,2) and failure in dealing with such events results in genomic instability. A key component of the DNA replication and repair machineries is the replication clamp PCNA. PCNA is a homotrimeric ring that is encoded by the *POL30* gene. It slides along the DNA during replication and serves as a docking platform for polymerases and other proteins that participate in DNA replication and repair processes (3). Additionally, PCNA undergoes post-translational modifications, such as ubiquitination and SUMOylation, during normal DNA replication and upon DNA damage. These modifications have a role in directing the cell toward one of the DNA damage bypass or repair pathways [reviewed in (3)]. Mono-ubiquitination of PCNA on lysine 164 by Rad6 and Rad18 promotes an error-prone Trans-Lesion Synthesis (TLS) repair pathway carried out by specific polymerases (4). Further poly-ubiquitination of the same residue by the E2 ubiquitin ligase Mms2/Ubc13 and the E3 ubiquitin ligase Rad5 summons an error-free damage bypass pathway that involves a transfer of information from the replicated chromatid (5,6). SUMOylation of PCNA K164 and/or K127 by the SUMO ligase Siz1 enhances the binding of the Srs2

---

*To whom correspondence should be addressed. Tel: +972-3-640-9031; Fax: +972-3-640-9407; Email: martin@post.tau.ac.il
Present addresses:
Marek Sebesta, Sir William Dunn School of Pathology, University of Oxford, South Parks Road, Oxford OX1 3RE, UK.
Martin Pacesa, Department of Biochemistry, University of Zurich, Winterthurerstrasse 190, CH-8057 Zurich, Switzerland.
Oren Parnas, Lautenberg Center for General and Tumor Immunology, BioMedical Research Institute Israel Canada of the Faculty of Medicine (IMRIC), The Hebrew University Hadassah Medical School, 91120 Jerusalem, Israel.

helicase, which disturbs Rad51 filament formation and thus inhibits homologous recombination (HR) (7–9).

The RFC complex, composed of a large subunit (Rfc1) and four small subunits (Rfc2–5), has the ability to load and unload PCNA onto DNA in an ATP-dependent manner (10). This activity is required at the firing of each origin of replication and for the formation of each Okazaki fragment on the lagging strand, as well as for efficient DNA repair. PCNA and its loader are essential and structurally conserved in all living organisms (11). In eukaryotic cells, three alternative clamp loaders (RFC-like complexes or RLCs) were identified. The RLCs share the four small subunits (Rfc2–5) of the canonical Rfc1 complex, but differ in the large subunit, which share homology with Rfc1. In yeast, the three identified RLCs are Elg1, Ctf18 and Rad24. These three alternative subunits are, in contrast to Rfc1, not essential for cell viability. Nevertheless, the RLCs have important roles in maintaining genomic stability (12,13). Ctf18 plays a role in sister chromatid cohesion, Rad24 is involved in the activation of the DNA damage checkpoint, and Elg1 has been implicated in many aspects of maintaining genomic stability (14–16). *ELG1* deletion results in increased sensitivity to genotoxic agents, elevated rates of spontaneous recombination, gross chromosomal rearrangements, loss of sister chromatid cohesion and elongated telomeres (13). Elg1 has been shown to interact genetically and physically with a variety of genes and proteins that are involved in DNA replication and repair, as well as with components of the SUMO pathway (17). The Elg1–RLC interacts with PCNA, particularly with its SUMOylated form, and has the ability to unload it from the chromatin (18–21). It has been recently shown that the unloading activity of the Elg1–RLC clamp is dependent on Okazaki fragment ligation (21), and that it occurs in S and G2/M phases of the cell cycle (22). The human orthologue of *ELG1*, ATAD5, has been shown to play a role in regulating the lifespan of DNA replication protein complexes by modulating PCNA levels on the chromatin (23). Homozygous ATAD5 mutations in mice are embryonically lethal, whereas over 95% of heterozygotes develop tumors. Moreover, mutations in ATAD5 were also found in several types of human cancers, implying a tumor-suppressing function for this gene (24). ATAD5 has been shown to be involved in the Fanconi Anemia DNA repair pathway by facilitating the de-ubiquitination of FANCI/FANCD2 heterodimer (25,26). The yeast Elg1 interacts both genetically and physically with the yeast orthologs of the Fanconi Anemia repair pathway (27).

Although it has already been established that Elg1 is an unloader of PCNA, it is still not clear whether the phenotypes of *elg1Δ* cells are a consequence of PCNA retention on the chromatin. To address this issue, we have used homology modeling to predict the structure of Elg1, and generated various mutants that vary in their PCNA unloading ability. By examining different phenotypes of the *elg1* mutants we found that the sensitivity of *elg1* mutants to DNA damage can be correlated with their ability to unload PCNA from the chromatin, and that the various roles of Elg1 in genome stability maintenance involve the unloading of both modified and unmodified PCNA. Our results also suggest a role for the retention of mono ubiquitinated PCNA on the chromatin in the suppression of MMS sensitivity of *rad5Δ* mutants by deletion of *ELG1*.

MATERIALS AND METHODS

Elg1 homology modeling

The Elg1 AAA+ region was modeled using similarity to the three-dimensional structure of Rfc1 from the yeast RFC–PCNA complex (PDB id: 1SXJ) (10). Elg1 and Rfc1 sequences were first aligned using pairwise comparison of corresponding profile hidden Markov models with HHsearch (28). The Elg1 structural model was then generated from the resulting sequence-structure alignment using Modeller (29). A model for Elg1 interaction with PCNA was obtained by overlaying the modeled Elg1 AAA+ region onto the Rfc1 subunit within the RFC–PCNA complex and subsequently removing the Rfc1 structure.

Yeast strains and plasmids

All yeast strains used are derivatives of MK166 (30), and are shown in Table 1. Mutants were created using standard yeast manipulation techniques. Yeast cells used in this study were grown at 30°C in either YPD medium or in Synthetic Dextrose (SD) medium supplemented with essential nutrients as required.

Site specific mutagenesis

A DNA fragment carrying full length *ELG*1::MYC marked with a *KAN*MX cassette was cloned into pGEM-T Easy Vector (Promega) and subjected to PCR using different forward and reverse primers containing the desired mutations (Table 2). Amplified PCR products were transformed into DH5α cells after digestion with Dpn1 (NEB). Plasmids were isolated and sequenced.

To transfer the mutation into the yeast genome, the mutagenized plasmids were digested with NotI (NEB) and transformed into *elg1*::*HphMX* cells. Transformed cells were selected on G418 plates. G418 resistant, hygromycin sensitive colonies were subjected to DNA sequencing to confirm the presence of the particular mutation, and the lack of spurious ones. In the *elg1-linker* allele the sequence of Elg1 between positions 289 and 320 was replaced by a five amino acid linker (Gly-Cys-Ala-Cys-Gly). The *elg1-SIM* mutant harbors the following mutations: I28A, I93K, II121,122AA.

Recombination rate assay

Recombination rates were measured as described previously (31), using the strain MK166 which allows to measure Ty recombination and DRR events.

Protein purification

Elg1–RLC and its mutant forms. Elg1–RLC was purified from *Saccharomyces cerevisiae* BJ5464 strain transformed with plasmids pBL448 (encoding *GST-ELG1* under control of *GAL1* promoter) and pBL422 (encoding *RFC2, RFC3, RFC4, RFC5* under control of *GAL1* promoter),

Table 1. Strains used in this study

Reference	Genotype	Strain name
(29)	*lys2:: TySup ade2-1(0c) can1-100 (0c) ura3-52 leu2-3,112 trp1del901 HIS3:: lys2:: ura3- his4::TRP1::his4*	MK166
This study	MK166 *elg1:HphMX*	MK10935
This study	MK166 ELG1-13Myc:: KanMX	MK11534
This study	MK166 *elg1-TT386/7AA*-13MYC:KanMX	*MK11880*
This study	MK166 *elg1-T386/7DD*-13MYC:KanMX	*MK11881*
This study	MK166 *elg1-I27A, I93K, III121,122AA*-13MYC:KanMX	*MK11240*
This study	MK166 *elg1-I27A, I93K, III121,122AA, TT386/7AA*-13MYC:KanMX	MK14904
This study	MK166 *elg1-I27A, I93K, III121,122AA, TT386/7DD*-13MYC:KanMX	MK14546
This study	MK166 *elg1-[289–319]* deletion and an insertion of GCACG-13MYC:KanMX	*MK15340*
This study	MK166 Rfc5-HA:HphMX	MK11293
This study	MK166 Rfc5-HA:HphMX, ELG1-13Myc::KanMX	MK13238
This study	MK166 Rfc5-HA:HphMX, *elg1-TT386/7AA*-13MYC:KanMX	MK13389
This study	MK166 Rfc5-HA:HphMX, *elg1-TT386/7DD*-13MYC:KanMX	MK13374
This study	MK166 Rfc5-HA:HphMX, *elg1-I27A, I93K, III121,122AA*-13MYC:KanMX	Mk11197
This study	MK166 Rfc5-HA:HphMX, *elg1-TT386/7AA, I27A, I93K, III121,122AA*-13MYC:KanMX	Mk15328
This study	MK166 Rfc5-HA:HphMX, *elg1-TT386/7DD, I27A, I93K, III121,122AA*-13MYC:KanMX	MK15532
This study	MK166 Rfc5-HA:HphMX, *[289–319]* deletion and an insertion of GCACG-13MYC:KanMX	MK15524
This study	MK166 *pol30-RR elg1:HphMX*	MK11938
This study	MK166 *pol30-RR* ELG1-13Myc:: KanMX	MK13396
This study	MK166 *pol30-RR elg1-TT386/7AA*-13MYC:KanMX	MK13394
This study	MK166 *pol30-RR elg1-TT386/7DD*-13MYC:KanMX	MK13398
This study	MK166 *pol30-RR elg1-I27A, I93K, III121,122AA*-13MYC:KanMX	MK13661
This study	MK166 *pol30-RR elg1-I27A, I93K, III121,122AA, TT386/7AA*-13MYC:KanMX	MK15402
This study	MK166 *pol30-RR elg1-I27A, I93K, III121,122AA, TT386/7DD*-13MYC:KanMX	MK15740
This study	MK166 *pol30-RR elg1-[282–319]* deletion and an insertion of GCACG-13MYC:KanMX	MK15438B
This study	MK166 *rad5:leu elg1:HphMX*	MK13081
This study	MK166 *rad5:LEU2* ELG1-13Myc:: KanMX	MK13078
This study	MK166 *rad5:LEU2 elg1-TT386/7AA*-13MYC:KanMX	MK11218B
This study	MK166 *rad5:LEU2 elg1-TT386/7DD*-13MYC:KanMX	MK15863
This study	MK166 *rad5:LEU2 elg1-I27A, I93K, III121,122AA*-13MYC:KanMX	MK13676
This study	MK166 *rad5:LEU2 elg1-I27A, I93K, III121,122AA, TT386/7AA*-13MYC:KanMX	MK15807
This study	MK166 *rad5:LEU2 elg1-I27A, I93K, III121,122AA, TT386/7DD*-13MYC:KanMX	MK14692
This study	MK166 *rad5:LEU2 elg1-[289–319]* deletion and an insertion of GCACG-13MYC:KanMX	MK15520
This study	MK166 *elg1:LEU2, rev3:URA3*	MK7212
This study	MK166 *rev3:URA3*	MK7218
This study	MK166 *elg1:LEU2, rev3:URA3, rad5:URA3*	MK7383
This study	MK166 *rev3:URA3rad5:URA3*	MK7392

Table 2. List of primers used to generate the Elg1 mutations through site directed mutagenesis

	Oligonucleotide	Sequence ($5' \to 3'$)
Elg1^{I93K}	Forward	ATGACGACGATGATGATCTTAAAGTAATCAGTGATAAGAGTCC
elg1-sim1	Reverse	GGACTCTTATCACTGATTACTTTAAGATCATCATCGTCGTCAT
Elg1^{II121,122AA}	Forward	AGCATGAAGATGATATTTCTGCCGCTTCCACATCGAGAATCAAATC
elg1-sim2,3	Reverse	GATTTGATTCTCGATGTGGAAGCGGCAGAAATATCATCTTCATGCT
Elg1^{TT386,387DD}	Forward	ATATCCTACTAGATTTTACCGACGACCACTATGTCAAAGATTCCTC
elg1-386/7DD	Reverse	GAGGAATCTTTGACATAGTGGTCGTCGGTAAAATCTAGTAGGATAT
Elg1^{TT386,387AA}	Forward	GATATCCTACTAGATTTTACCGCCGCACACTATGTCAAAGATTCC
elg1-386/7AA	Reverse	GGAATCTTTGACATAGTGTGCGGCGGTAAAATCTAGTAGGATATC
Elg1^{linker}	Forward	CTACCTTGAGGAACCGTCTATTGAACAGAATAAATGGTTGTGCATGTGGC
elg1-linker	Reverse	GGAACAAATTCGCTCAAGCTGCTATTTGCTTCGCCGCCACATGCACAACC

which were generously provided by Peter Burgers, according to the protocol of (32) with minor modifications. Briefly, a fresh overnight culture was diluted 8-fold in fresh synthetic medium lacking tryptophan and uracil, and containing galactose (2%, w/v), glycerol (3%) and lactic acid (3%) and was incubated for 22–24 h at 30°C with shaking. Cells were harvested by centrifugation and stored at −80°C.

Elg1–RLC and its mutants were purified as follows: 70–100 g of yeast paste was lysed by cryo-milling. The resulting powder was dissolved in 200 ml of lysis buffer C, consisting of 50 mM Tris–HCl (pH 7.5), 10% sucrose (w/v), EDTA (10 mM), dithiothreitol (3 mM), nonidet-P40 (0.01%, v/v), NaCl (150 mM) and protease inhibitors (aprotinin, chymostatin, leupeptin, pepstatin A, benzamidine, each at 5 μg/ml). Solid ammonium sulphate was then added to the lysate to a final concentration of 300 mM and the mixture was stirred for 25 min at 4°C. Afterward, 45 μl of 10% Polymin P per 1 ml of the lysate was added, and the mixture

was gently stirred at 4°C for 10 min. The crude lysate was clarified by centrifugation (100 000 × g for 90 min). Next, Elg1–RLC complex was precipitated from the cleared lysate using ammonium sulphate (0.35 g/ml), and the precipitate was kept overnight at −80°C. The next day, the precipitate was dissolved in buffer T (25 mM Tris–Cl, 10% (v/v) glycerol, 5 mM EDTA, pH 7.5). The conductivity of the sample was adjusted to be equal of buffer T containing 150 mM NaCl and mixed with 2 ml of glutathione sepharose, equilibrated in the same buffer. After 2–3 h at 4°C, the beads were washed with 150 ml of buffer T, containing 150 mM NaCl. GST-Elg1–RLC was eluted with buffer T, containing 150 mM NaCl, supplemented with 20 mM glutathione (reduced form) and 0.05% ampholytes. Fractions containing the complex were pooled and incubated for 3 h at 4°C with 5–15 μg of PreScission protease. Elg1–RLC complex was then loaded onto 1 ml MonoS column equilibrated with buffer T containing 100 mM NaCl and 0.05% ampholytes.

After 10 ml wash with buffer T containing 100 mM NaCl, 0.05% ampholytes, 5 mM $MgCl_2$ and 100 μM ATP, the complex was eluted with 20 ml linear gradient of 100–500 mM NaCl. Fractions containing Elg1–RLC were pooled and concentrated in a Vivaspin concentrator and stored in 2 μl aliquots at $-80°$C.

PCNA and Polymerase δ purification.   PCNA and the polymerase δ complex were expressed and purified using the procedure described previously (33).

RFC complex purification.   The RFC complex was purified from *Escherichia coli* using the procedure described by (34)

D-loop extension assay

The D-loop assay was performed essentially as described previously (35). Briefly, the fluorescent D1 oligonucleotide (90-mer; 3 μM nucleotides) was incubated for 5 min at 37°C with Rad51 (1 μM) in 10 μl buffer R (35 mM Tris–HCl pH 7.4, 2 mM ATP, 2.5 mM $MgCl_2$, 50 mM KCl, 1 mM DTT and ATP regenerating system consisting of 20 mM creatine phosphate and 20 μg/ml creatine kinase). Rad54 (150 nM) was added to the reaction in 1 μl, followed by a 3 min incubation at 23°C. The reaction was initiated by addition of the pBluescript replicative form I (50 μM base pairs) in 1.5 μl and incubated for 5 min at 23°C.

The primer extension reaction was assembled as described in Sebesta *et al.* (33). Briefly, a standard 30 μl reaction mixture containing 12 μl from the D-loop reaction was supplemented with 660 nM RPA, 10 nM PCNA or SUMO-PCNA, 0.3 nM RFC and 33 nM Polδ in buffer O (20 mM Tris–HCl pH 7.5, 5 mM DTT, 0.1 mM EDTA, 150 mM KCl, 40 μg/ml BSA, 8 mM $MgCl_2$, 5% glycerol and 75 μM each of dGTP and dCTP). PCNA loading reaction was incubated at 30°C for 5 min. The reaction was stopped by cooling on ice followed by addition of increasing concentrations (10, 50, 250 nM) of Elg1–RLC. Alternatively and where indicated, Srs2 (20 nM) and other indicated proteins (Ulp1, 15 nM) where incorporated. The reaction was continued at 30°C for an additional 5 min. DNA synthesis was initiated by addition of buffer O containing 75 μM dTTP and 0,375 μCi [α-^{32}P] dATP. After 10 min extension at 30°C, the reactions were stopped, deproteinized and loaded onto a 0.8% (w/v) agarose gel. The gel was either directly analyzed for fluorescent DNA species or dried on DE81 paper and exposed to a Phosphorimager screen and imaged in Fuji FLA 9000 imager with the Multi Gauge software (36).

ΦX-based extension assay

The assay was performed essentially as described in (37). The reaction (20 μl final volume) was assembled on single primed ΦX174 virion ssDNA (5 nM) in buffer O (20 mM Tris–Cl pH 7.5, 5 mM DTT, 0.1 mM EDTA, 70 mM KCl, 0.5 mM ATP, 40 μg/ml BSA, 8 mM $MgCl_2$, 5% glycerol and 60 μM each of dGTP and dCTP), in the presence of RPA (1 μM), PCNA (10 nM), RFC (17.5 nM), Pol δ (5 nM) followed by a 5 min incubation at 30°C to allow loading of PCNA on the substrate. DNA synthesis was initiated by adding the start buffer (60 μM dTTP and 0.375 μCi [α-32P]dATP in buffer O). After the indicated time at 30°C, the reactions were stopped with SDS (0.5% final) and Proteinase K (0.5 mg/ml) and loaded onto an agarose gel (0.8% (w/v)). After electrophoresis, the gel was dried on DE81 paper, exposed to phosphorimager screen, scanned in Fuji FLA 9000 imager and analyzed with the Multi Gauge software (Fuji).

DNA damage sensitivity

Serial 10-fold dilutions of logarithmic yeast cells were spotted on fresh SD-complete plates with or without MMS and incubated at 30°C for 3 days.

To calculate relative MMS resistance, all the strains were plated at the same MMS concentration (0.025% for the *POL30 RAD5* background; 0.008% for the *pol30-RR RAD5* background and 0.0012% for the *POL30 rad5Δ* background) such that individual colonies (20–200 per plate) could be obtained and counted after 3 days at 30°C. Three to six individual cultures were tested this way. The Resistance Coefficient of each mutant is the ratio between the average number of colonies in plates with MMS and the average number of colonies obtained in plates without MMS, divided by the results observed in the wt control.

Chromatin fractionation assay

Cells from 50 ml cultures ($OD_{600} < 1.0$) were collected by centrifugation, successively washed with ddH_2O, PSB (20 mM Tris–Cl pH 7.4, 2 mM EDTA, 100 mM NaCl, 10 mM b-ME) and SB (1 M Sorbitol, 20 mM Tris–Cl pH 7.4), and transferred to a 2 ml ependorff tube. Cells were suspended in 1 ml SB, 30 μl Zymolase 20T (20 mg/ml in SB) was added, and samples were incubated at 30°C with rotation until >85% spheroplasts were observed (60–90 min). Spheroplasts were collected by centrifugation (2K, 5 min, 4°C), washed twice with SB, and suspended in 500 ml EBX (20 mM Tris–Cl pH 7.4, 100 mM NaCl, 0.25% Triton X-100, 15 mM β-ME + protease/phosphatase inhibitors). Triton X-100 was added to a 0.5% final concentration to lyse the outer cell membrane, and the samples kept on ice for 10 min with gentle mixing. An aliquot was taken for western blot analysis (WCE), and the remainder of the lysate was layered over 1 ml NIB (20 mM Tris–Cl pH 7.4, 100 mM NaCl, 1.2 M sucrose, 15 mM β-ME + protease/phosphatase inhibitors) and centrifuged at 12K RPM for 15 min, at 4°C. A sample of the upper cytoplasmic layer fraction was taken for Western blot analysis (cytoplasm) and the rest of the supernatant was discarded. The glassy white nuclear pellet was suspended in 500 μl EBX and Triton X-100 was added to a 1% final concentration to lyse the nuclear membrane. The chromatin and nuclear debris were collected by centrifugation (15K, 10 min, 4°C). Chromatin was suspended in 50 μl Tris pH 8.0 for western blot analysis (Chromatin). To each fraction an equal volume of 2× SDS-PAGE loading buffer (60 mM Tris pH 6.8, 2% SDS, 10% glycerol, 0.2% bromophenol blue, 200 mM DTT) was added, samples were incubated at 95°C for 5 min and sonicated at 80%, 5 cycles, 10 s per cycle. Samples were analyzed by SDS-PAGE and western blot analyses.
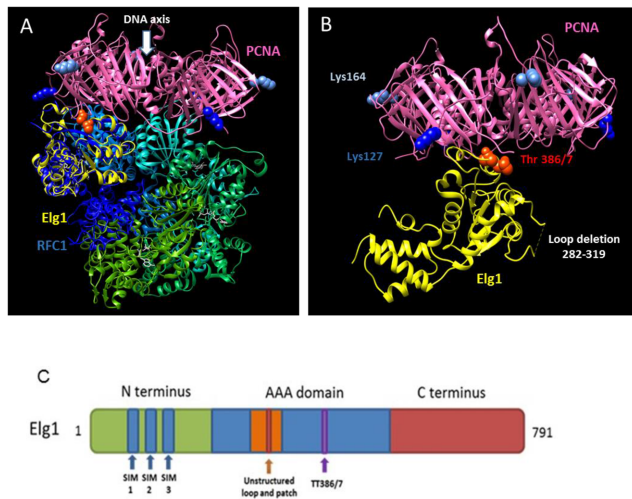
Figure 1. Homology modeling of the Elg1 central region. (**A**) A side view of the RFC complex subunits (colored from blue to green) with PCNA (pink). A model of the Elg1 AAA+ region (yellow) is predicted according to the homology with Rfc1 (blue). (**B**) A prediction of the interaction site between Elg1 AAA+ region and PCNA. Lysines 127 and 164 of PCNA are indicated. The *elg1-sim* mutations, located at Elg1's N-terminus, is not displayed here. (**C**) A schematic representation of the Elg1 protein and the generated point mutations.

Western blotting

Western blotting and quantification were performed as described previously. Antibodies used for Western blotting were mouse monoclonal anti-PCNA diluted 1:1000 in 5% skim milk (ab70472, Abcam), rabbit polyclonal anti-histone H3 diluted 1:5000 in 5% skim milk (ab46765, Abcam), rabbit polyclonal anti RPS6 diluted 1:1000 in 5% BSA (ab40820, Abcam), mouse monoclonal anti MYC diluted 1:1000 in 5% skim milk (sc-40 Santa Cruz) Monoclonal Mouse anti-actin diluted 1:5000 in 5% skim milk (ab3280, Abcam). The western results were quantified using ImageJ software; at least three blots were used for each calculation.

RESULTS

Homology modeling of Elg1 to identify novel mutation sites

In order to investigate the relationship between Elg1–RLC mediated PCNA unloading and genomic instability, we first generated a predicted structural model of the yeast Elg1 protein. All subunits of the RFC clamp loader complex (Rfc1–5) contain an AAA+ ATPase domain, that is required for PCNA loading [reviewed in (38)]. Elg1's AAA+ ATPase domain is believed to be inactive (39), but it bears a sequence and structure similarity to the Rfc1 AAA+ domain. Taking advantage of the previously published crystal structure of the RFC complex together with PCNA (10,40), we were able to construct a homology model of Elg1's central AAA+ domain structure and its complex with PCNA (Figure 1A–C). Based on this structural model we marked several regions for mutagenesis (Figure 1C):

1) Threonines 386/7 in Elg1 correspond to asparagines 694 and 695 of the human Rfc1, which were shown to be

involved in the interaction between Rfc1 and the C-terminal region of PCNA (40). These two threonine residues were mutated to differently charged amino acids: either aspartic acid (hereby referred to as *elg1-386/7DD* mutant) or to alanines (*elg1-386/7AA* mutant). By introducing these mutations we expected to reduce the strength of interaction between Elg1 and PCNA and therefore to disturb Elg1's clamp unloading activity.

2) An unstructured loop, spanning from aa 290 to aa 319, containing a hydrophobic patch. This loop is conserved throughout all Elg1 orthologs but is absent in other components of the RFC complex and in the other Rfc1-like proteins (Ctf18 and Rad24). An unstructured loop with a hydrophobic patch is a possible protein-protein interaction site and therefore we deleted this region to identify functions unique to the Elg1–RLC, replacing it with a short flexible linker (see Materials and Methods). We hereafter refer to this allele as *elg1-linker*.

3) Putative SUMO interaction motifs (SIMs) within the N-terminal domain of Elg1 were shown to affect the interaction between Elg1 and SUMOylated PCNA (19). Mutations in these motifs are likely to disrupt the interaction of Elg1 with the SUMO moiety, but not other interactions (19). The point mutations are located at the following positions: SIM1: I28A, SIM2: I93K, SIM3: II121,122AA.

4) Finally, we combined the *elg1-sim* and *TT386/387* alleles; these alleles are referred to as *elg1-sim+386/7AA* and *elg1-sim+386/7DD*. In these alleles, we expect the interactions with both PCNA and SUMO to be disrupted.

Corresponding isogenic strains carrying MYC tagged versions of wt or mutant *elg1* alleles were generated, at the normal genomic loci and under regulation of the endogenous promoter. The Elg1 protein level remains unchanged in different *elg1* alleles compared to the wt (Supplementary Figure S1A). Next, we performed co-IP and showed that the interaction between the various Elg1 alleles and the RFC small subunits is also not altered in the mutants (Supplementary Figure S1B). Hence, any phenotypic change caused by these mutations is not a consequence of reduced protein expression or a reduced formation of the Elg1–RLC complex. This conclusion is further supported by the fact that all mutations presented here are recessive and the MMS sensitivity of these strains can be fully complemented by a centromeric plasmid carrying the wt *ELG1* allele (Supplementary Figure S1C).

Elg1 mutants accumulate varying levels of PCNA on the chromatin

Cumulative results from several laboratories suggest that the main role of the Elg1–RLC is to unload PCNA and indeed, *elg1Δ* cells accumulate PCNA on chromatin (18–20,23). As PCNA can be post-translationally modified, various types of PCNA modifications can be distinguished according to their electrophoretic mobility [(18,19,41,42), Supplementary Figure S1D]. In *elg1Δ*, the increased accumulation of SUMOylated PCNA is the most dramatic (∼50-fold increase, compared to only 3-fold increase in accumulation of unmodified PCNA (Figure 2). Fractionation experiments revealed large differences in the ability
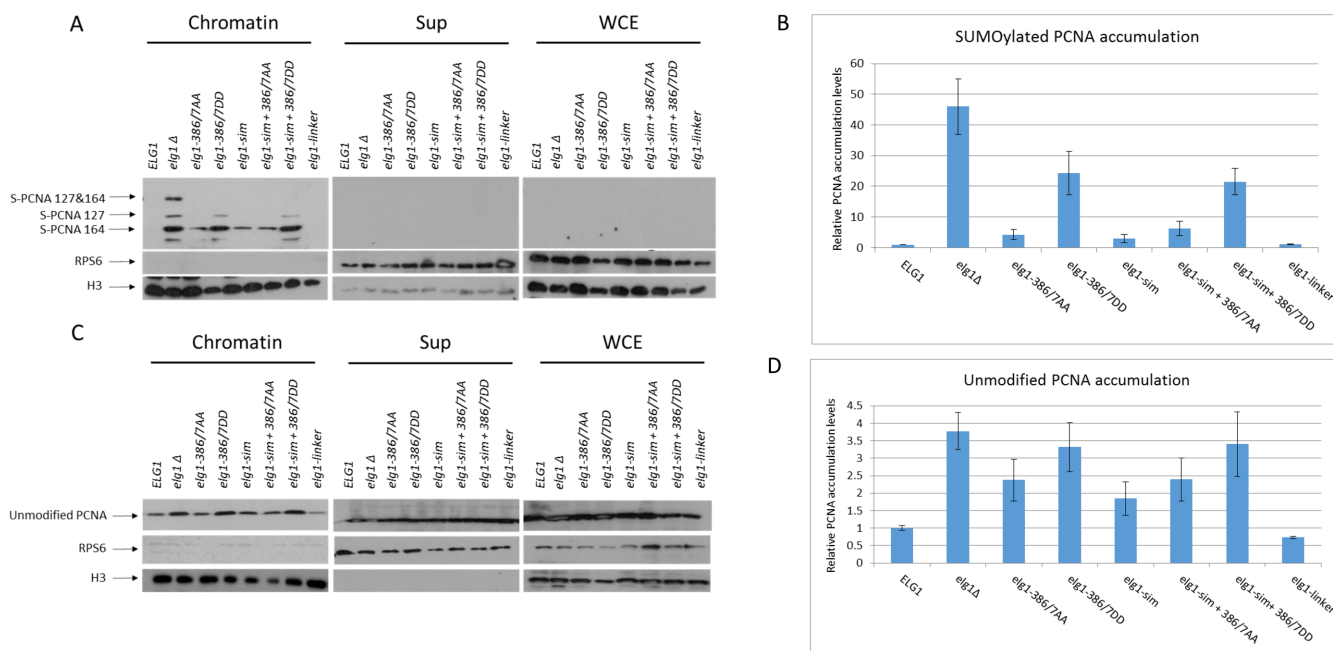
Figure 2. *elg1* mutants exhibit variability in PCNA unloading. A fractionation assay followed by western blot to detect PCNA levels shows different modified (**A** and **B**) and unmodified (**C** and **D**) PCNA levels on the chromatin in the various *elg1* mutants in MK166 strain background. Histone H3 and RPS6 served as chromatin-bound and unbound controls. Histone H3 levels were also used as a loading control. At least 3 experiments were used for quantitation and the error bars represent the standard error of the mean.

of the various *elg1* mutants to unload PCNA from chromatin: The *elg1-386/7AA* mutant accumulates only a small amount of PCNA on the chromatin, suggesting that this mutant retains most of Elg1's unloading ability. In contrast, the *elg1-386/7DD* mutant accumulates a larger proportion of both SUMOylated and unmodified PCNA on the chromatin. When the three SIM motifs in the N-terminal domain of Elg1 are mutated (*elg1-sim*), a very mild accumulation of both modified and unmodified PCNA is observed on the chromatin (Figure 2). The double mutant *elg1-sim + 386/7DD* is as defective in PCNA unloading as the *elg1-386/7DD* allele, which shows that the SIM motifs are not only mediating the interaction of Elg1 with the SUMO moiety attached to PCNA, but are also important for the interaction with PCNA itself, either directly (by changing the affinity of Elg1 to PCNA) or indirectly (by interacting with another SUMOylated protein to stabilize the interaction and promote the unloading process). In contrast to these results, the *elg1-linker* mutant appears completely proficient in PCNA unloading, and did not accumulate any form of PCNA on the chromatin (Figure 2).

After determining the PCNA unloading activity of each of the point mutants, we investigated whether it correlates with the severity of the mutants' phenotypes

Point mutations in Elg1 impinge on its ability to inhibit *in vitro* DNA synthesis

Since Elg1–RLC preferentially unloads SUMOylated PCNA from the chromatin during DNA replication (18,21), we asked whether a similar biochemical activity is also necessary for DNA repair. Furthermore, we wished to study the activity of Elg1 *in vitro* using a purified

complex. We therefore modified an already existing *in vitro* repair/replication system [Figure 3A; (33,43)]. In our assay, Pol δ synthesizes DNA using a D-loop as primer, successfully recapitulating the DNA synthesis step required in all homology-dependent repair/tolerance pathways (44,45) (Figure 3A, upper panel). Importantly, we have successfully used this assay to determine that the Srs2 helicase dissociates the complex between SUMO–PCNA and Polymerase (Pol) δ, thereby regulating the length of extension products during PCNA-dependent DNA repair synthesis (33). The known mechanism of action of Srs2 in the assay served as a unique control for our experiments with Elg1–RLC. In this assay, addition of Elg1–RLC together with SUMO–PCNA resulted in a reproducible 5-fold reduction in DNA synthesis (Figure 3A, compare lanes 9 and 12), which did not occur upon addition of unmodified PCNA to the reaction (Figure 3A, compare lanes 5 and 8), suggesting that Elg1–RLC unloads SUMO–PCNA *in vitro*. To further corroborate the role of SUMO, we tested whether the presence of Ulp1, a SUMO-specific protease that deSUMOylates proteins, together with Elg1–RLC, would reverse the observed inhibition. As shown in Supplementary Figure S2A, addition of Ulp1 resulted in restoration of DNA synthesis, suggesting that Elg1–RLC indeed acted preferentially upon SUMOylated PCNA.

Elg1–RLC also efficiently inhibited DNA synthesis in the well-defined ΦX-174 system (37) in the presence of SUMO-PCNA (Supplementary Figure S2B), suggesting that the Elg1–RLC PCNA unloading activity is independent of the substrate tested, and therefore relevant for both DNA repair and DNA replication.
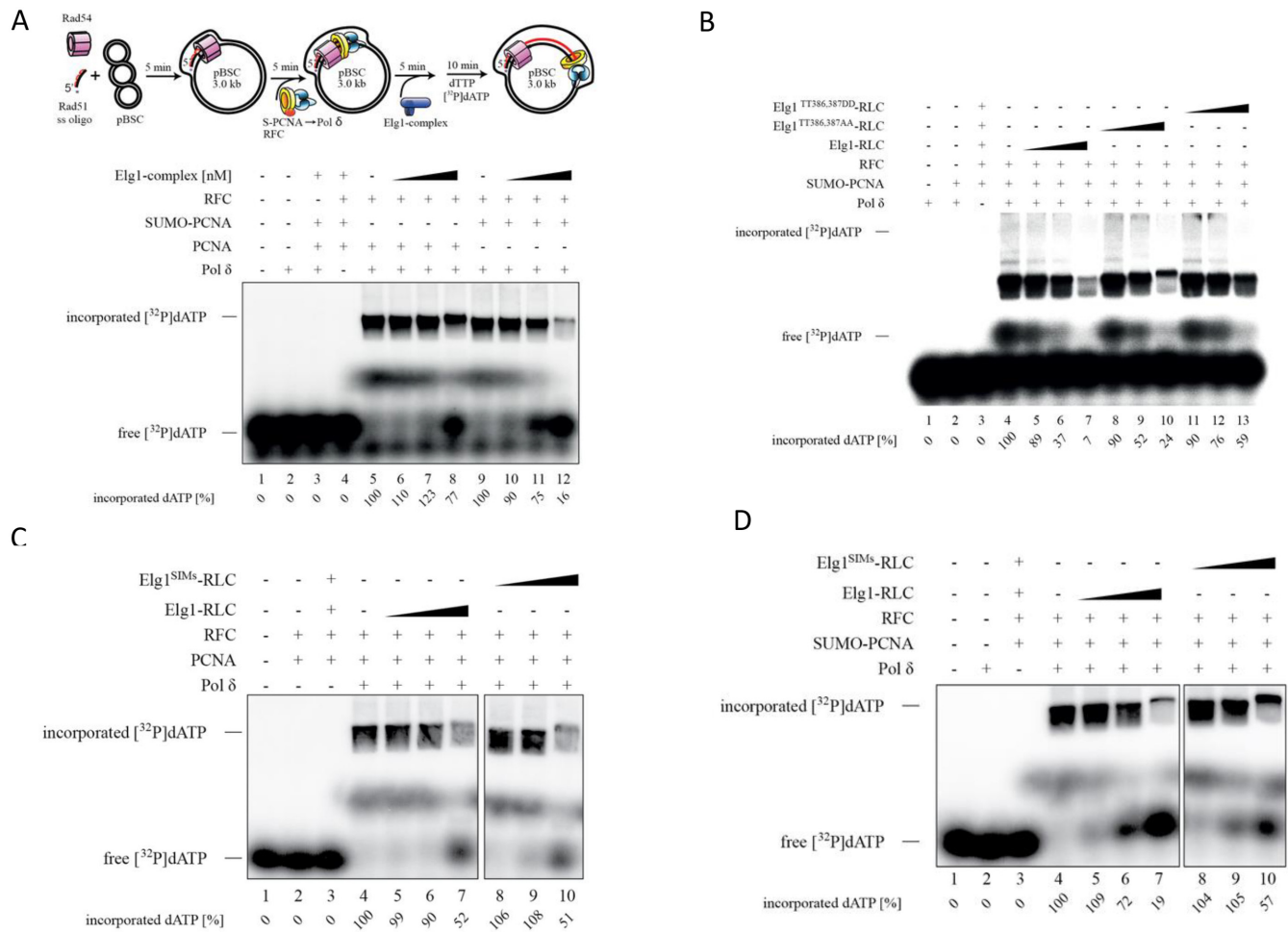
Figure 3. Elg1 mutants affect DNA synthesis *in vitro*. (**A**) Upper panel. Schematic representation of the reaction. (see Materials and Methods). Lower panel. Elg1–RLC inhibits DNA synthesis *in vitro,* preferentially in the presence of SUMOylated PCNA. (**B**) *elg1-386/7AA* mutant complex inhibits DNA synthesis in the presence of SUMOylated PCNA, whereas *elg1-386/7DD* complex is defective in the inhibition. (**C**) *elg1-sim* is proficient in inhibiting DNA synthesis in the presence of unmodified PCNA. (**D**) *elg1-sim* is only partially proficient in inhibiting DNA synthesis in the presence of SUMO–PCNA.

Srs2 inhibits DNA synthesis by dissociating the DNA polymerase from the reaction (33). To test the mode of action of Elg1, we carried out order-of-addition experiments (Supplementary Figure S2C and D). Both Srs2 and the Elg1–RLC complex inhibit DNA synthesis *in vitro* (Supplementary Figure S2C, lane 9 and Supplementary Figure S2D, lane 9). When SUMO–PCNA remains on the DNA, an addition of the de-SUMOylating enzyme Ulp1 after the action of Srs2 restarts DNA synthesis (Supplementary Figure S2B, lane 13), as Srs2 has 7-fold lower affinity to PCNA over SUMO–PCNA (46). In contrast, when an analogous experiment was performed with Elg1–RLC, we observed no restart of DNA synthesis when Ulp1 was added alone (Supplementary Figure S2A, lane 13). Only when increasing concentrations of the RFC complex were added along with Ulp1, did we observe restart of DNA synthesis. These results are in line with the model in which Elg1–RLC unloads SUMO–PCNA from DNA and thus more RFC complex is needed in order to reload it and allow further DNA synthesis *in vitro*.

Interestingly, at high Elg1–RLC concentrations a small decrease in mobility of the band that represents the reaction product (e.g.: Figure 3A, lane 8) can be observed. This observation points to the possibility that Elg1–RLC may interact with the free PCNA in the reaction, reducing the amount of free PCNA that is able to compete for Polymerase δ binding, and resulting in longer DNA synthesis tracks.

Next, we compared the mutants known to accumulate PCNA on chromatin in this *in vitro* assay. While *elg1-386/7AA* mutant alleles showed a minor inhibition of *in vitro* DNA synthesis, the addition of the *elg1-386/7DD* protein did not inhibit DNA synthesis (Figure 3B), suggesting that this mutant is unable to unload SUMO-PCNA. These results correlate with the PCNA accumulation data and show that the different *elg1* mutants inhibit DNA synthesis *in vitro* in accordance with their PCNA unloading capabilities *in vivo*.

The *elg1-sim* mutant had the same inhibitory effect on DNA synthesis in the presence of unmodified PCNA as the wt Elg1 (Figure 3C, lanes 7 and 10), but when SUMO–PCNA was added to the reaction, the inhibition by *elg1-sim* was not as high as by wt Elg1 (Figure 3D, lanes 7 and 10). This is in accordance with the role of the SIM motives as

mediators of the interaction of Elg1 with the SUMO moiety attached to PCNA.

The sensitivity of *elg1* mutants to DNA damage correlates with their PCNA accumulation status

In order to determine the significance of PCNA accumulation in genomic stability, we tested the sensitivity of various *elg1* mutants to DNA damage. MMS (Methyl Methanesulfonate) is a DNA damaging agent that causes DNA methylation. When compared to the *elg1 Δ* allele, the *elg1-386/7AA, elg1-sim* and *elg1-linker* mutants are resistant to MMS whereas the *elg1-386/7DD* mutant exhibits an intermediate sensitivity to MMS. The double *elg1-sim+386/7DD* mutant is as sensitive to DNA damage as the *elg1Δ* strain, showing an additive effect for the SIM motifs and the PCNA interaction site mutations regarding DNA damage sensitivity (Figure 4A). In order to better quantify the effect of the various mutations on the sensitivity to DNA damaging agents, we devised a Resistance Coefficient (RC) parameter (see Materials and Methods for details). In brief, all mutants and the wt strain were diluted and plated on plates without or with 0.025% MMS, and the survival on MMS was calculated for each strain, normalized by comparing it to the survival of the wt. When the RC value is plotted against the relative PCNA accumulation value (derived from the fractionation assays followed by a western blot), a clear correlation can be observed. Figure 4C and D show that the MMS resistance of the *elg1* mutants is tightly correlated with both the SUMOylated and unmodified PCNA accumulation status of these mutants ($R^2 = 0.81$· and 0.90, respectively). Very similar results were obtained with 4-nitroquinoline 1-oxide (4-NQO), a DNA damaging agent that forms bulky adducts (47) (Figure 4B). Taken together, these results support a model in which the DNA damage sensitivity of *elg1Δ* cells is caused by PCNA accumulation on the chromatin.

The high recombination rates of *ELG1* mutants are dependent on the PCNA unloading activity

It has been reported that *elg1Δ* cells exhibit high rates of homologous recombination [HR; (19,31)]. Using MK166, a strain in which different types of recombination events can be monitored, we measured the rate of direct repeat recombination (DRR) and non-reciprocal recombination between Ty elements (gene conversion) (30) (see Materials and Methods and Figure 5A). As previously described (31), *elg1Δ* strains exhibit a greatly increased rate of HR (∼5-fold increased for DRR, ∼18-fold for Ty recombination). The DRR and Ty recombination rates of the *elg1-386/7AA* and *elg1-sim* mutants are comparable to those of the wt strain, whereas in the *elg1-386/7DD* mutant the Ty recombination rate is intermediate and the DRR rate is similar to that of *elg1Δ*. Combining the SIM mutations with the *386/7* replacements results again in an additive effect, as in the DNA damage sensitivity assay, and the rates of Ty recombination and DRR of the double mutant *elg1-sim+386/7DD* are close to those seen in the strain harboring a complete *ELG1* deletion. The *elg1-linker* mutation did not affect the levels of homologous recombination (Figure 5B). Thus, we

could see a strong correlation between the rates of recombination and the level of unmodified or SUMOylated PCNA accumulation ($R^2 = 0.80$ and 0.88, respectively; Figure 5C and D). Our results show that the *elg1* mutants that accumulate more PCNA on the chromatin are more sensitive to DNA damage and have higher recombination rates and thus PCNA accumulation correlates with genomic instability.

The MMS sensitivity of *elg1Δ* is related to unmodified PCNA unloading

PCNA can undergo ubiquitination at lysine 164, and SUMOylation at lysines 127 and 164 (3). *pol30-KK164,127RR* (hereafter referred to as *pol30-RR*) is a mutant allele of PCNA in which these two critical lysines are mutated to an arginine, preventing post translational modifications.

We tested various mutant *elg1* alleles in the background of the *pol30-RR* mutation in order to determine the importance of PCNA modifications for the activity of the Elg1–RLC (Figure 6). Significantly, the *elg1Δ* mutation increases the sensitivity to MMS of a *pol30-RR* mutant, implying that part of the *elg1Δ* phenotype is independent of PCNA modifications (Figure 6A).

The MMS sensitivity of the mutants in a *pol30-RR* background shows the same gradient of sensitivities as in the *POL30* background (Figure 4A), with a general shift towards more severe sensitivity: the *elg1-386/7DD* mutant is as sensitive as *elg1Δ, elg1-386/7AA* is less severe than *elg1-386/7DD* but more sensitive than the wt. The *elg1-sim* and *elg1-linker* mutations show no MMS sensitivity, and combining the 386/7 mutations with the SIM mutations resulted in an additive phenotype: the *pol30-RR elg1-sim+386/7AA* mutant shows a more severe phenotype than the single mutants and the *pol30-RR elg1-sim+386/7DD* combination shows a sensitivity as high as that of the *pol30-RR elg1Δ* double mutant. The unmodified PCNA accumulation level in the different *elg1* mutant strains varies in the *pol30-RR* background according to the same gradient that was observed in the wt background: *elg1-386/7DD* and *elg1-sim+386/7DD* mutants accumulate unmodified PCNA at levels similar to those seen in the *elg1Δ pol30-RR* double mutant. *elg1-386/7AA, elg1-sim* and *elg1-sim+386/7AA* accumulate only a small amount of unmodified PCNA and the *elg1-linker* mutants do not accumulate unmodified PCNA at all. Thus, the correlation between DNA damage sensitivity and PCNA accumulation is not affected by mutations that preclude PCNA modification ($R^2 = 0.847$; Figure 6C).

Taken together, our results show that the phenotypic variation observed among the *elg1* mutants correlates with the amount of PCNA that is retained on the chromatin, irrespectively of its modification status.

Suppression of the DNA damage sensitivity of *rad5Δ* mutants

Another interesting phenotype of *elg1Δ* is its suppression of the sensitivity to MMS of the *rad5Δ* mutant (19). *RAD5* is best known as an E3 ubiquitin ligase that poly-ubiquitinates PCNA in response to DNA damage, together with the E2
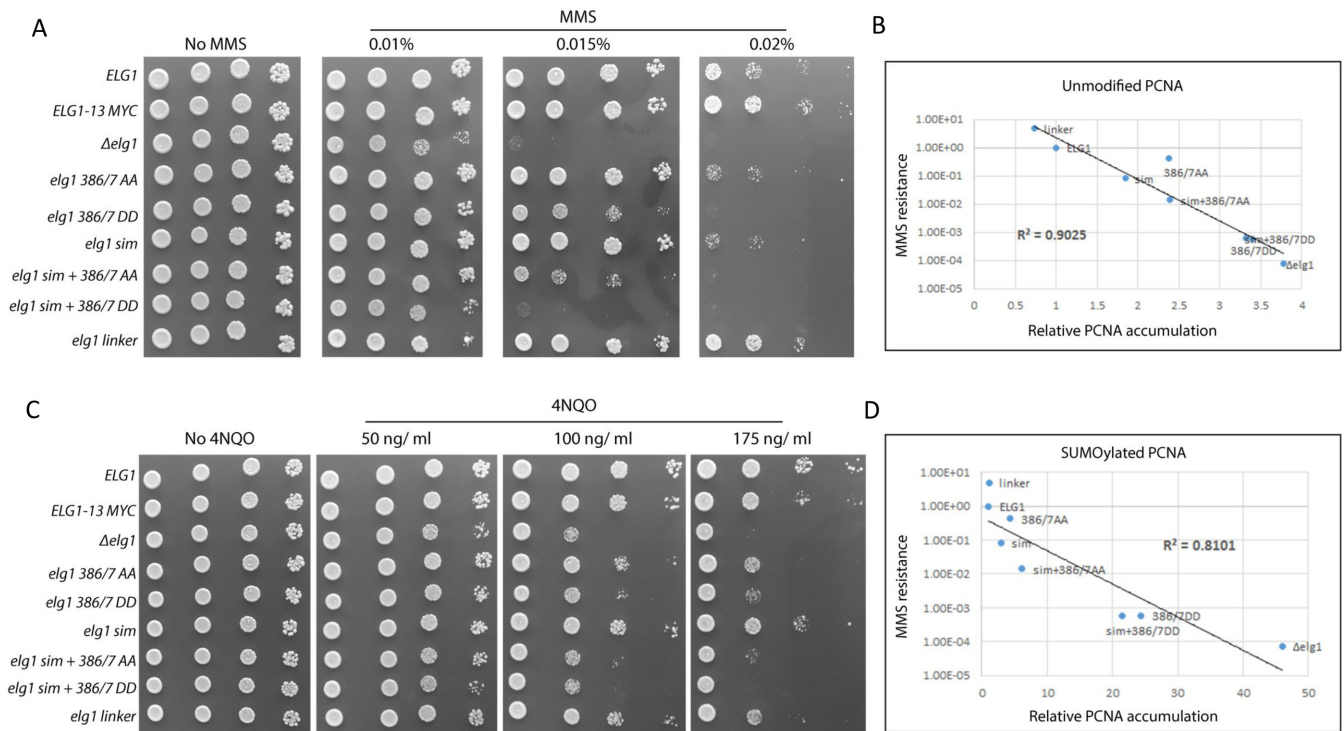
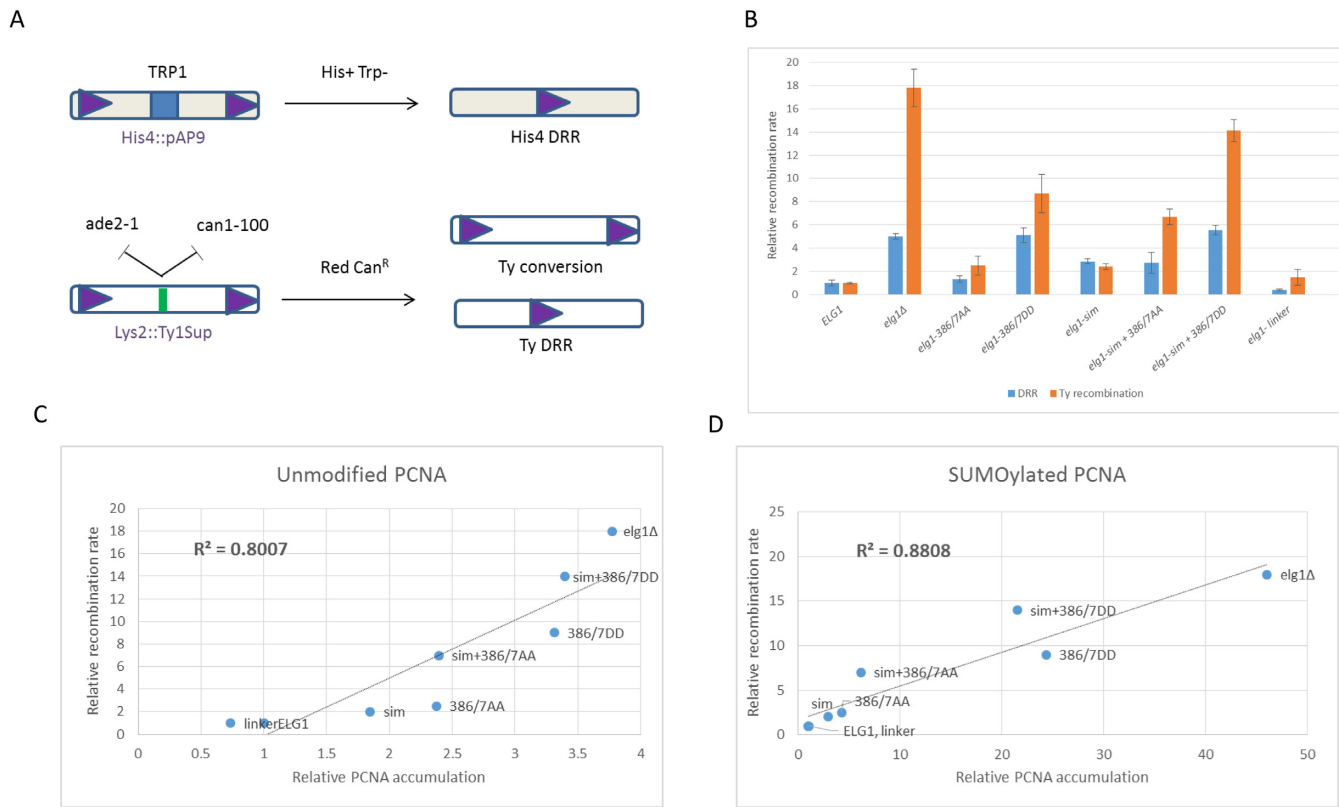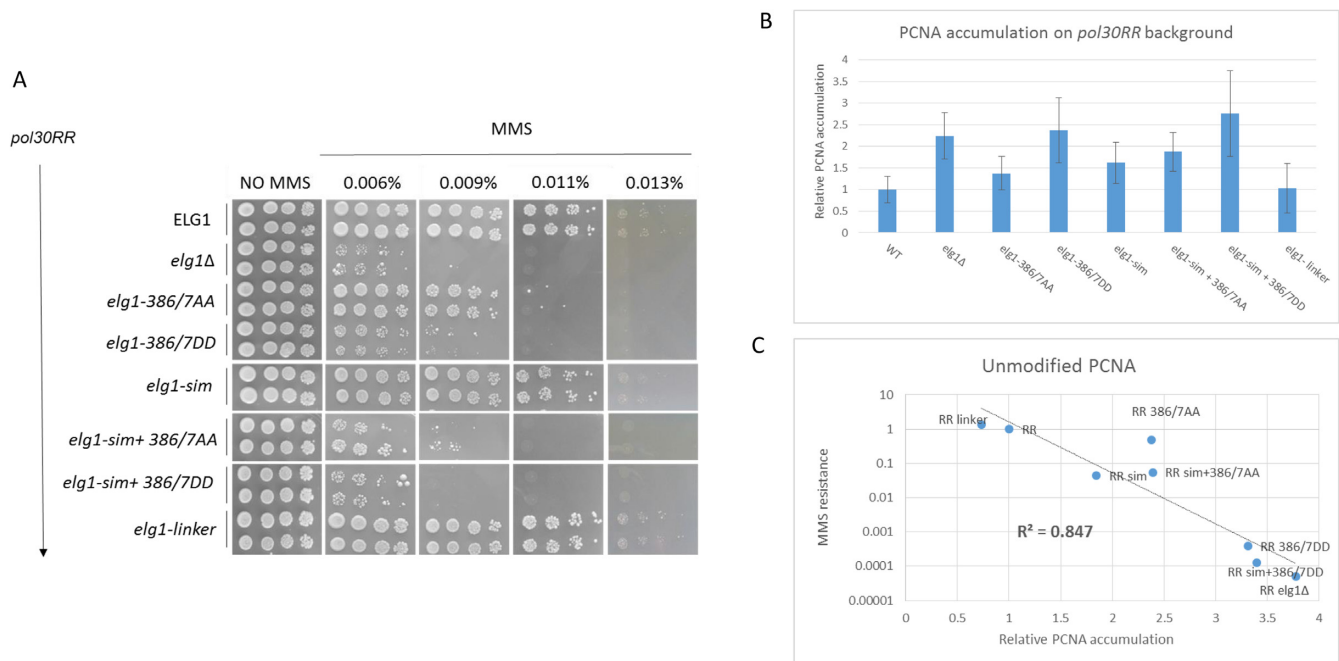**Figure 4.** DNA damage sensitivity of *elg1* mutants correlate with PCNA accumulation. (**A** and **C**) Serial dilutions of yeast cultures on minimal SD-complete plates with or without methylmethane sulphonate (MMS) or 4-nitroquinoline 1-oxide (4-NQO) in the indicated concentration show different sensitivities of *elg1* mutants in MK166 strain. (**B** and **D**) The MMS resistance coefficient calculated from a plating assay plotted against unmodified and SUMOylated PCNA accumulation, respectively.

Mms2/Ubc13 (48,49). Poly-ubiquitination of PCNA occurs sequentially after mono ubiquitination by the SUMO-dependent Ubiquitin ligase Rad18 (50) and is required to direct the cell towards an error-free lesion bypass pathway. In addition, Rad5 has an helicase activity that has been suggested to reverse fork progression (51). *rad5Δ* cells are very sensitive to MMS and a deletion of *ELG1* partially suppresses this high sensitivity. *ELG1* deletion was shown to specifically suppress the MMS sensitivity caused by defects in the E3 ubiquitin ligase activity of Rad5 (19). The mechanism by which a deletion of *ELG1* suppresses *rad5Δ* MMS sensitivity and the PCNA modification status that is required to allow this suppression effect is unclear. We decided to approach this question by trying to correlate the PCNA unloading activity and the ability of the different *ELG1* mutations to suppress the MMS sensitivity of *rad5Δ*. With the exception of the *elg1-linker* allele, which seems to retain the full activity of wt Elg1, all the other mutations suppress *rad5Δ* MMS sensitivity to the same extent as the *elg1Δ* allele (Figure 6A). Strains deleted for *RAD5* accumulate suppressors at a very high rate and therefore it was challenging to perform fractionation assays; Figure 6B shows that the accumulation of unmodified PCNA of *elg1* mutants in the absence of *RAD5* was similar to that seen in the *RAD5* background, with the *elg1-386/7DD* and *elg1-sim+386/7DD* mutants showing the highest levels. Interestingly, the SUMOylated fraction of PCNA, which is usually much less prominent than the unmodified fraction, was not consistently detected in *rad5Δ* mutants regardless of the *ELG1* allele in the strain (see Discussion). The RC scores

for unmodified PCNA accumulation levels in the various mutants in the presence of MMS in the *rad5Δ* background showed no correlation ($R^2 = 0.052$) with MMS sensitivity (Figure 6C). The almost-universal suppression of *rad5Δ* by *elg1* alleles can be interpreted in two ways (see model in Figure 8C): (i) Reduced Elg1–RLC activity leads to both modified and unmodified PCNA accumulation. In the absence of the error free DNA repair pathway the SUMOylated PCNA that is retained on the chromatin recruits the Srs2 helicase (8) and thus causes an inhibition of the HR pathway. However, the unmodified or the mono-ubiquitinated PCNA that is retained on the chromatin is enough to enable a pathway that can partially bypass the DNA damage sensitivity, and this is achieved in all the mutants tested, with the exception of the *elg1-linker* allele, which seems to retain the full capacity of PCNA unloading of wt Elg1 (Figure 6B and C). (ii) Alternatively, the suppression of the MMS sensitivity phenotype of *rad5Δ* mutants is a consequence of another activity of Elg1 that is not related to PCNA unloading, and which is abolished by all the mutations except for the *elg1-linker* mutant. We prefer the first option, which is more parsimonious. In addition, we have recently found that mutations which prevent Elg1 phosphorylation upon DNA damage (S6,8,112A and S,6,8,112E) suppress the MMS sensitivity of *rad5Δ*, even when, in a *RAD5* genetic background, they show no MMS sensitivity (52). The large number of independent mutants with partial or total reduction of Elg1 PCNA unloading activity that are able to suppress the DNA damage sensitivity of *rad5Δ* mutants suggests that an accu-

Figure 5. Recombination rates of *elg1* mutants are correlated with PCNA accumulation. (**A**) A schematic representation of the MK166 recombination levels monitoring system. (**B**) Recombination rates were calculated for various *elg1* mutants by plating the MK166 yeast strain on selective media (see Materials and Methods). (**C** and **D**) The recombination rates plotted against unmodified and SUMOylated PCNA accumulation, respectively.

Figure 6. The sensitivity to MMS in the various mutants is not dependent on PCNA modifications. (**A**) Serial dilutions of yeast cultures on minimal SD-complete plates with or without MMS in the indicated concentrations show different sensitivities of *elg1* mutants to MMS in MK166 *pol30-RR* background. (**B**) PCNA levels on the chromatin of the same strains. (**C**) The RC in a *pol30-RR* background correlates with the ability of the different *elg1* mutants to unload PCNA.
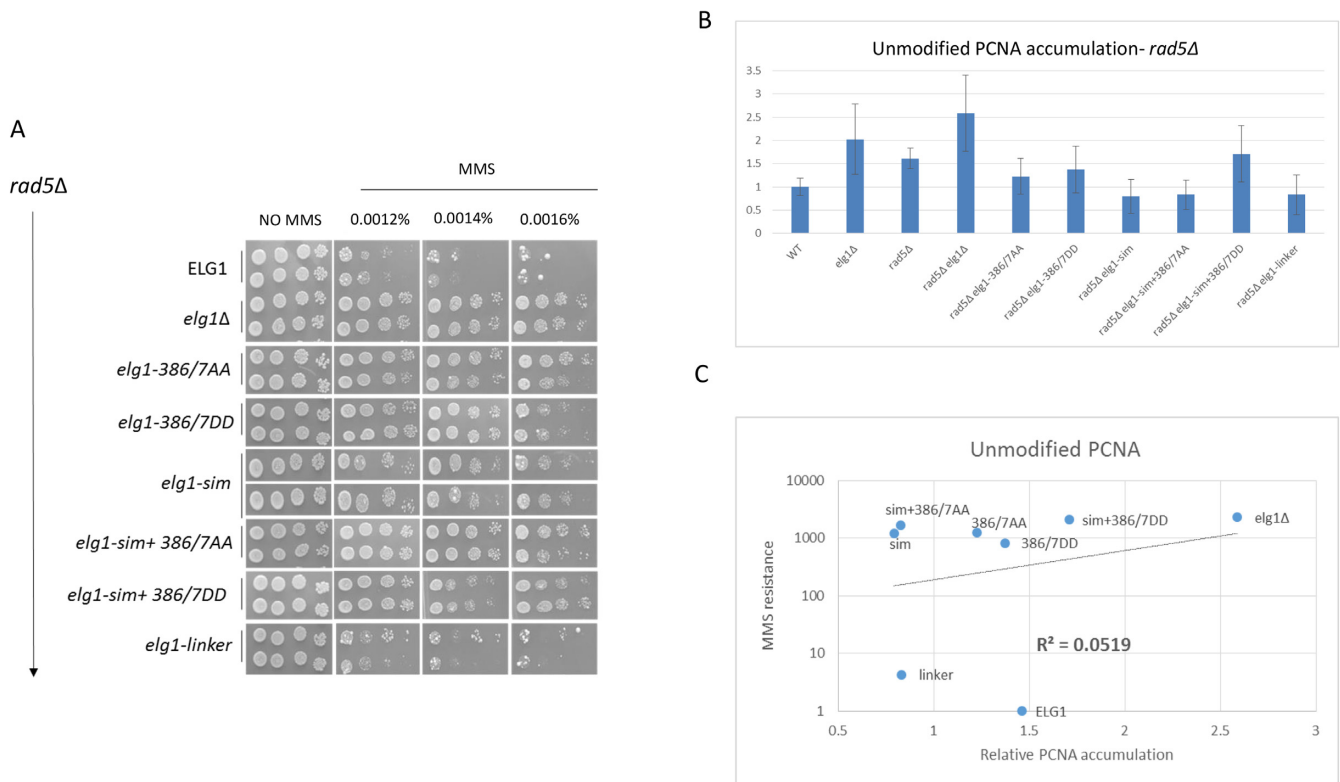
Figure 7. *elg1* mutants suppress *rad5Δ* MMS sensitivity. (**A**) Serial dilutions of yeast cultures on minimal SD-complete plates with or without MMS at the indicated concentrations show suppression of MK166 *rad5Δ* MMS sensitivity by all of the mutants except for *elg1-linker*. (**B**) Unmodified PCNA levels on the chromatin in the various *elg1* mutants in the *rad5Δ* background. (**C**) The RC in *rad5Δ* background does not correlate with the ability of the different *elg1* mutants to unload PCNA.

mulation of a low level of PCNA that is not SUMOylated is sufficient to alleviate this suppression phenotype.
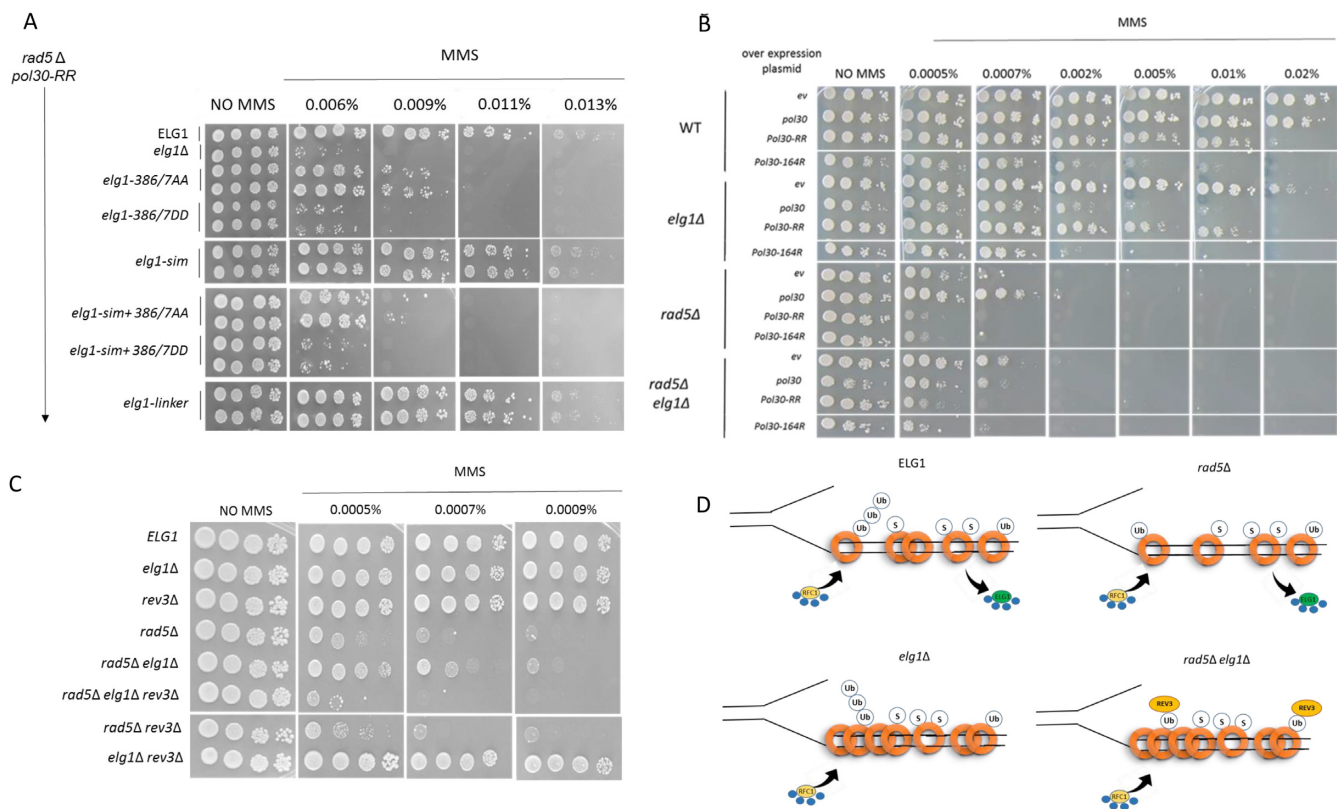
Suppression of the MMS sensitivity of *rad5Δ* mutants requires PCNA modification

To further understand the mechanism that suppresses the sensitivity of *rad5Δ* mutants when *ELG1* is deleted, we introduced all the *elg1* mutations into a *rad5Δ pol30-RR* background, in which PCNA cannot be modified, and tested the ability of the various strains to grow in the presence of MMS. The *pol30-RR* allele suppresses the *rad5Δ* MMS sensitivity (to the level of resistance observed in the single *pol30-RR*) showing that the MMS sensitivity of *rad5Δ* is due to PCNA modification. Importantly, deletion of *ELG1* had the same additive effect with the *pol30-RR* allele in the double mutant *pol30-RR rad5Δ* background and in the single *pol30-RR* background, and so did the various *elg1* alleles (compare Figures 6A and 8A). This implies that while PCNA modifications are a pre-requisite for *rad5Δ* MMS sensitivity (there is no sensitivity if PCNA is not modified), the level of PCNA unloading by Elg1–RLC has a different phenotypic effect that depends on the PCNA modification status (in a modifiable PCNA background all *elg1* alleles have the same effect, whereas a gradient of phenotypes is seen when PCNA is unmodified).

To directly test the effect of PCNA accumulation on the chromatin and the PCNA modifications required to allow

elg1Δ suppression of *rad5Δ* MMS sensitivity, we overexpressed three PCNA alleles: modifiable wt *POL30*, the unmodifiable *pol30-RR* allele, or a PCNA allele that cannot be ubiquitinated (*pol30-164R*), in wt, *elg1Δ*, *rad5Δ* and *rad5Δ elg1Δ* mutant strains (Figure 8B). It has been shown (22,53), that PCNA overexpression causes an accumulation of PCNA on the chromatin. Overexpression of *pol30-RR* confers slight MMS sensitivity to both wt and *elg1Δ* strains. However, whereas overexpression of *POL30* has no effect on the wt strain, it leads to increased sensitivity in the *elg1Δ* strain; this is consistent with the accumulation of PCNA being responsible for the MMS sensitivity: when Elg1–RLC is active, some of the PCNA can be removed from the chromatin; when it is inactive (in *elg1Δ* strains), PCNA accumulates even more. Interestingly, the slight sensitivity conferred by the overexpression of *pol30-RR* is similar whether Elg1 is present or absent, showing again a preference of the Elg1–RLC for unloading SUMOylated PCNA (19).

Consistent with the idea that PCNA modifications are required for *elg1Δ* suppression of the MMS sensitivity of *rad5Δ*, overexpression of neither *pol30-RR* nor *pol30-164R* suppresses the sensitivity of a *rad5Δ* mutant. Only the overexpression of modifiable *POL30* is able to suppress the MMS sensitivity of *rad5Δ* (Figure 8B). These results suggest that lysine 164, the target of mono-ubiquitination, is essential for the suppression of *rad5Δ*. The suppression effect of *pol30-164R* overexpression is epistatic to the effect caused by deletion of *ELG1*, again supporting the idea that the sup-

Figure 8. *elg1Δ* suppression of *rad5Δ* MMS sensitivity depends on PCNA modifications. (**A**) Serial dilutions of yeast cultures on minimal SD-complete plates with or without MMS at the indicated concentrations show different sensitivities of *elg1* mutants to MMS in MK166 *pol30-RR rad5Δ* background. (**B**) An overexpression plasmid of *POL30*, *pol30-RR* or *pol30-164R* alleles was introduced into the indicated strains and the MMS sensitivity of these strains was tested. (**C**) A deletion of *REV3* abolishes the suppression effect of *elg1Δ* on *rad5Δ* MMS sensitivity. (**D**) A schematic representation of the model proposed: in wt cells the Elg1 RLC unloads PCNA from the DNA. This may take place during DNA repair or during DNA replication. Poly-ubiquitination of PCNA by Rad5 allows error-free repair. In the absence of *ELG1*, PCNA accumulates and becomes modified, mainly by SUMOylation. In *rad5Δ* cells, the error-free post-replication bypass mechanism triggered by PCNA poly-ubiquitination is eliminated, leading to sensitivity to DNA damage. In the absence of both *RAD5* and *ELG1* the TLS damage bypass pathway, mediated by PCNA mono ubiquitination and Rev3, can operate.

pression of *rad5Δ* by deletion of Elg1 is due to the accumulation of mono- ubiquitinated PCNA. Accordingly, over-expression of PCNA that cannot be ubiquitinated (either *pol30-164R* or *pol30-RR*) abolishes the suppression effect conferred by *elg1Δ* in the *rad5Δ* background (Figure 8B). In contrast to the almost full suppression observed in *rad5Δ siz1Δ* or *rad5Δ srs2Δ* double mutants (8,17,54), which are explained by the availability of HR as an alternative repair mechanism in the absence of the error-free Rad5-initiated bypass pathway, deletion of *ELG1* has a milder effect, which can be explained by the use of the less efficient trans-lesion synthesis (error-prone) pathway upon accumulation of low levels of mono-ubiquitinated PCNA. Mono-ubiquitination of PCNA enables the recruitment of trans-lesion synthesis polymerases, such as Rev3 (PolZeta) [reviewed in (3)].

In order to test that hypothesis we deleted *REV3* in the *rad5Δ elg1Δ* background. As expected, ablation of the trans-lesion synthesis polymerase abolished the suppression effect of *elg1Δ* on *rad5Δ* (Figure 8C). We therefore conclude that the suppressive effect of *elg1* mutations in the *rad5Δ* background is caused by accumulation of mono-ubiquitinated PCNA on the chromatin, which partially rescues *rad5Δ* hyper sensitivity phenotype in a *REV3*- dependent manner.

DISCUSSION

In this paper, we have investigated the correlation between the Elg1's clamp unloading activity, the accumulation of modified and unmodified PCNA on the chromatin, and genomic instability. In order to do so we generated a set of mutations in designated regions with a differential ability to unload PCNA from the chromatin.

By predicting the structure of Elg1's central domain we identified threonines 386 and 387 as residues that might mediate the interaction between PCNA and Elg1. The strains that contain mutations in these residues exhibit a retention of PCNA on the chromatin. It was previously reported that Elg1 contains a distorted PIP motif in the N terminal domain. This motif, however, showed no effect on DNA damage sensitivity nor on the actual interaction with PCNA (39). It was recently shown (55) that the PIP motives of various proteins mediate the interaction of the protein with partners other than PCNA, and we suspect that this could be the case in the Elg1 putative PIP motif.

We have also mutated a unique unstructured loop containing a hydrophobic patch that is conserved among *ELG1* orthologs but not in other Rfc1-like proteins. Surprisingly, deletion of this loop had no noticeable phenotype and the

mutants were able to carry out all the known activities of Elg1 at wt levels. The function of this loop thus remains unknown.

All previous *in vitro* work with Elg1 was carried out with Elg1–RLC immunoprecipitated from yeast cells. Here we show for the first time, using purified proteins, that the Elg1 complex inhibits DNA synthesis, by a mechanism that is different from that shown for the Srs2 helicase (33): Whereas Srs2 interacts with SUMOylated PCNA and dissociates it from the DNA polymerase, the Elg1–RLC unloads the modified PCNA altogether (Figure 3 and Supplementary Figure S2C and D).

We have tested the PCNA accumulation status of the mutants and discovered a gradient of accumulation levels, which reflects the capacity of the various mutants to unload PCNA from chromatin (Figure 2). A striking correlation was found between the PCNA unloading ability and genomic instability phenotypes such as: MMS sensitivity, 4-NQO sensitivity and the recombination frequency of the *elg1* mutant strains. This correlation suggests that the sensitivity to DNA damage and the increased recombination rate in *elg1* mutants are the consequence of the retention of PCNA on the chromatin, probably through the inappropriate recruitment of interacting partners that are important for choosing the repair mechanism or the processing of recombination intermediates.

ELG1 is not an essential gene; in its absence PCNA is eventually unloaded by alternative mechanisms and therefore either the physical accumulation of the clamps for an extended period of time or the delay in completing DNA replication cause genome instability.

What form of PCNA (modified or unmodified) is responsible for the phenotypes of *elg1* mutants? Abolishing PCNA modifications (by using *pol30-RR* allele) caused a sensitization of all the *elg1* mutants in a way that retained these mutant's graduated differential DNA damage sensitivity phenotype observed in the *POL30* background (Figure 4). Thus, PCNA modification is not a pre-requisite for the enhanced MMS sensitivity of *elg1* mutants. While this paper was in review, Johnson and co-workers presented additional evidence that the MMS sensitivity of *elg1Δ* is a consequence of PCNA retention on the chromatin (22). Taken together, our results fit a model in which PCNA SUMOylation functions as a hallmark of PCNA retention and its levels build up when PCNA is not unloaded from the chromatin by the Elg1 complex. Since PCNA requires proximity or attachment to DNA in order to get SUMOylated (42), it is possible that the accumulation of SUMOylated PCNA on the chromatin is time-dependent, and thus more SUMOylated proteins are seen on the chromatin as a function inversely proportional to the activity of the various *elg1* mutants.

Paradoxically, we see that the suppressive effect of *elg1* mutations on *rad5Δ* requires PCNA modification. Except for the *elg1-linker* mutants, all the other mutants were able to suppress the MMS sensitivity conferred by deletion of *RAD5*. Previously, several groups have shown that the sensitivity of *rad5Δ* mutants to genotoxic agents can be suppressed either by preventing PCNA SUMOylation (by using the *pol30-RR* allele or deleting *SIZ1*), or by deleting the helicase *SRS2* (8,17,54). The current model thus proposes that the MMS sensitivity of *rad5Δ* strains is caused by PCNA SUMOylation that indirectly prevents the cells from repairing DNA damage by HR. The suppression of *rad5Δ* by mutations in *ELG1* is milder than that seen in the absence of PCNA SUMOylation or Srs2, and it was unclear what is the precise mechanism by which it takes place. As most *elg1* mutants tested in this study, and in a recently published one (52) show full suppression, irrespectively of the position of the mutation or of the severity of the unloading defect, it appears that a minor accumulation of PCNA provides a threshold above which the suppression can occur. Since the only allele that failed to suppress the sensitivity of a *rad5Δ* strain is the *elg1-linker* allele, which displays wild type levels of PCNA unloading activity, the suppression effect seems related to the clamp unloading activity of Elg1. Overexpression experiments (Figure 8B) showed that the suppression requires modifiable, and specifically mono-ubiquitinated, PCNA. which would allow lesion bypass by recruiting a trans-lesion synthesis polymerase (56). Indeed, deletion of *REV3,* the gene encoding the main trans-lesion synthesis polymerase in yeast, abolished the suppression conferred by deletion of *ELG1* (Figure 8C). Previous genetic results indeed showed that *rad5Δ* mutants exhibit high levels of mutagenesis, which depend both on the TLS polymerase encoded by *REV3* and on the mono-ubiquitination activity of the *RAD18* gene (57). Interestingly, whereas a single copy of the *pol30-RR* allele in the genome suppresses the sensitivity of *rad5Δ* mutants (compare Figures 7A and 8A) and similar results are observed when wt *POL30* is overexpressed (Figure 8B), overexpression of *pol30-RR* and of *pol30-164R* (in the presence of a wt genomic PCNA copy) failed to show such effect, even in the absence of Elg1–RLC activity. These results imply that the sensitivity of *rad5Δ* to MMS is due to the presence of SUMOylated PCNA; if the only copy of PCNA present cannot be modified, a reduced sensitivity to genotoxins is seen. This is consistent with our model (Figure 8D): In wt cells, lesions are repaired in an error-free manner by the *RAD5* pathway, enabled by poly-ubiquitination of PCNA. In the absence of the Rad5-initiated bypass mechanism, recruitment of Srs2 to SUMOylated PCNA causes sensitivity, as it prevents an alternative repair by HR. Deletion of *ELG1* suppresses the high sensitivity of *rad5Δ* mutants by delaying PCNA unloading, allowing more mono-ubiquitinated PCNA to remain on the chromatin, and thus enabling the recruitment of the Rev3 trans-lesion synthesis polymerase (Figure 8D).

In conclusion, our work shows that modified and unmodified PCNA have a variety of roles in conferring genome stability and these roles are greatly affected by the activity of Elg1-RFC clamp unloader.

SUPPLEMENTARY DATA

Supplementary Data are available at NAR Online.

ACKNOWLEDGEMENTS

REFERENCES

1. Zeman,M.K. and Cimprich,K.A. (2014) Causes and consequences of replication stress. *Nat. Cell Biol.*, **16**, 2–9.
2. Yeeles,J.T., Poli,J., Marians,K.J. and Pasero,P. (2013) Rescuing stalled or damaged replication forks. *Cold Spring Harbor Perspect. Biol.*, **5**, a012815.
3. Gazy,I. and Kupiec,M. (2012) The importance of being modified: PCNA modification and DNA damage response. *Cell Cycle*, **11**, 2620–2623.
4. Ulrich,H.D. (2004) How to activate a damage-tolerant polymerase: consequences of PCNA modifications by ubiquitin and SUMO. *Cell Cycle*, **3**, 15–18.
5. Xu,X., Blackwell,S., Lin,A., Li,F., Qin,Z. and Xiao,W. (2015) Error-free DNA-damage tolerance in Saccharomyces cerevisiae. *Mut. Res. Rev. Mut. Res.*, **764**, 43–50.
6. Minca,E.C. and Kowalski,D. (2010) Multiple Rad5 activities mediate sister chromatid recombination to bypass DNA damage at stalled replication forks. *Mol. Cell*, **38**, 649–661.
7. Lytle,A.K., Origanti,S.S., Qiu,Y., VonGermeten,J., Myong,S. and Antony,E. (2014) Context-dependent remodeling of Rad51-DNA complexes by Srs2 is mediated by a specific protein-protein interaction. *J. Mol. Biol.*, **426**, 1883–1897.
8. Papouli,E., Chen,S., Davies,A.A., Huttner,D., Krejci,L., Sung,P. and Ulrich,H.D. (2005) Crosstalk between SUMO and ubiquitin on PCNA is mediated by recruitment of the helicase Srs2p. *Mol. Cell*, **19**, 123–133.
9. Krejci,L., Van Komen,S., Li,Y., Villemain,J., Reddy,M.S., Klein,H., Ellenberger,T. and Sung,P. (2003) DNA helicase Srs2 disrupts the Rad51 presynaptic filament. *Nature*, **423**, 305–309.
10. Bowman,G.D., O'Donnell,M. and Kuriyan,J. (2004) Structural analysis of a eukaryotic sliding DNA clamp-clamp loader complex. *Nature*, **429**, 724–730.
11. Park,S.Y., Jeong,M.S., Han,C.W., Yu,H.S. and Jang,S.B. (2015) Structural and functional insight into proliferating cell nuclear antigen. *J. Microbiol. Biotechnol.*
12. Majka,J. and Burgers,P.M. (2004) The PCNA-RFC families of DNA clamps and clamp loaders. *Prog. Nucleic Acids Res. Mol. Biol.*, **78**, 227–260.
13. Aroya,S.B. and Kupiec,M. (2005) The Elg1 replication factor C-like complex: a novel guardian of genome stability. *DNA Repair (Amst.)*, **4**, 409–417.
14. Majka,J. and Burgers,P.M. (2003) Yeast Rad17/Mec3/Ddc1: a sliding clamp for the DNA damage checkpoint. *Proc. Natl. Acad. Sci. U.S.A.*, **100**, 2249–2254.
15. Hanna,J.S., Kroll,E.S., Lundblad,V. and Spencer,F.A. (2001) Saccharomyces cerevisiae CTF18 and CTF4 are required for sister chromatid cohesion. *Mol. Cell. Biol.*, **21**, 3144–3158.
16. Mayer,M.L., Gygi,S.P., Aebersold,R. and Hieter,P. (2001) Identification of RFC(Ctf18p, Ctf8p, Dcc1p): an alternative RFC complex required for sister chromatid cohesion in S. cerevisiae. *Mol. Cell*, **7**, 959–970.
17. Parnas,O., Amishay,R., Liefshitz,B., Zipin-Roitman,A. and Kupiec,M. (2011) Elg1, the major subunit of an alternative RFC complex, interacts with SUMO-processing proteins. *Cell Cycle*, **10**, 2894–2903.
18. Kubota,T., Nishimura,K., Kanemaki,M.T. and Donaldson,A.D. (2013) The Elg1 Replication Factor C-like Complex Functions in PCNA Unloading during DNA Replication. *Mol. Cell*, **50**, 273–280.
19. Parnas,O., Zipin-Roitman,A., Pfander,B., Liefshitz,B., Mazor,Y., Ben-Aroya,S., Jentsch,S. and Kupiec,M. (2010) Elg1, an alternative subunit of the RFC clamp loader, preferentially interacts with SUMOylated PCNA. *EMBO J.*, **29**, 2611–2622.
20. Shiomi,Y. and Nishitani,H. (2013) Alternative replication factor C protein, Elg1, maintains chromosome stability by regulating PCNA levels on chromatin. *Genes Cells*, **18**, 946–959.
21. Kubota,T., Katou,Y., Nakato,R., Shirahige,K. and Donaldson,A.D. (2015) Replication-coupled PCNA unloading by the Elg1 complex occurs genome-wide and requires Okazaki fragment ligation. *Cell Rep.*, **12**, 774–787.
22. Johnson,C., Gali,V.K., Takahashi,T.S. and Kubota,T. (2016) PCNA retention on DNA into G2/M phase causes genome instability in cells lacking Elg1. *Cell Rep.*, **16**, 684–695.
23. Lee,K.Y., Fu,H., Aladjem,M.I. and Myung,K. (2013) ATAD5 regulates the lifespan of DNA replication factories by modulating PCNA level on the chromatin. *J. Cell Biol.*, **200**, 31–44.
24. Bell,D.W., Sikdar,N., Lee,K.Y., Price,J.C., Chatterjee,R., Park,H.D., Fox,J., Ishiai,M., Rudd,M.L., Pollock,L.M. *et al.* (2011) Predisposition to cancer caused by genetic and functional defects of mammalian Atad5. *PLoS Genet.*, **7**, e1002245.
25. Lee,K.Y., Yang,K., Cohn,M.A., Sikdar,N., D'Andrea,A.D. and Myung,K. (2010) Human ELG1 regulates the level of ubiquitinated proliferating cell nuclear antigen (PCNA) through Its interactions with PCNA and USP1. *J. Biol. Chem.*, **285**, 10362–10369.
26. Kee,Y. and D'Andrea,A.D. (2010) Expanded roles of the Fanconi anemia pathway in preserving genomic stability. *Genes Dev.*, **24**, 1680–1694.
27. Singh,S., Shemesh,K., Liefshitz,B. and Kupiec,M. (2013) Genetic and physical interactions between the yeast ELG1 gene and orthologs of the Fanconi anemia pathway. *Cell Cycle*, **12**.
28. Soding,J. (2005) Protein homology detection by HMM-HMM comparison. *Bioinformatics*, **21**, 951–960.
29. Webb,B. and Sali,A. (2014) Comparative protein structure modeling using MODELLER. *Curr. Protoc. Bioinformatics*, **47**, 5 6 1-32.
30. Liefshitz,B., Parket,A., Maya,R. and Kupiec,M. (1995) The role of DNA repair genes in recombination between repeated sequences in yeast. *Genetics*, **140**, 1199–1211.
31. Ben-Aroya,S., Koren,A., Liefshitz,B., Steinlauf,R. and Kupiec,M. (2003) ELG1, a yeast gene required for genome stability, forms a complex related to replication factor C. *Proc. Natl. Acad. Sci. U.S.A.*, **100**, 9906–9911.
32. Bylund,G.O., Majka,J. and Burgers,P.M. (2006) Overproduction and purification of RFC-related clamp loaders and PCNA-related clamps from Saccharomyces cerevisiae. *Methods Enzymol.*, **409**, 1–11.
33. Sebesta,M., Burkovics,P., Haracska,L. and Krejci,L. (2011) Reconstitution of DNA repair synthesis in vitro and the role of polymerase and helicase activities. *DNA Repair (Amst.)*, **10**, 567–576.
34. Finkelstein,J., Antony,E., Hingorani,M.M. and O'Donnell,M. (2003) Overproduction and analysis of eukaryotic multiprotein complexes in Escherichia coli using a dual-vector strategy. *Anal. Biochem.*, **319**, 78–87.
35. Krejci,L., Macris,M., Li,Y., Van Komen,S., Villemain,J., Ellenberger,T., Klein,H. and Sung,P. (2004) Role of ATP hydrolysis in the antirecombinase function of Saccharomyces cerevisiae Srs2 protein. *J. Biol. Chem.*, **279**, 23193–23199.
36. Scher,J., Wankiewicz,E., Brown,G.M. and Fujieda,H. (2003) AII amacrine cells express the MT1 melatonin receptor in human and macaque retina. *Exp. Eye Res.*, **77**, 375–382.
37. Langston,L.D. and O'Donnell,M. (2008) DNA polymerase delta is highly processive with proliferating cell nuclear antigen and undergoes collision release upon completing DNA. *J. Biol. Chem.*, **283**, 29522–29531.
38. Duderstadt,K.E. and Berger,J.M. (2008) AAA+ ATPases in the initiation of DNA replication. *Crit. Rev. Biochem. Mol. Biol.*, **43**, 163–187.
39. Davidson,M.B. and Brown,G.W. (2008) The N- and C-termini of Elg1 contribute to the maintenance of genome stability. *DNA Repair (Amst.)*, **7**, 1221–1232.
40. Venclovas,C., Colvin,M.E. and Thelen,M.P. (2002) Molecular modeling-based analysis of interactions in the RFC-dependent clamp-loading process. *Protein Sci.*, **11**, 2403–2416.

41. Hoege,C., Pfander,B., Moldovan,G.L., Pyrowolakis,G. and Jentsch,S. (2002) RAD6-dependent DNA repair is linked to modification of PCNA by ubiquitin and SUMO. *Nature*, **419**, 135–141.

42. Parker,J.L., Bucceri,A., Davies,A.A., Heidrich,K., Windecker,H. and Ulrich,H.D. (2008) SUMO modification of PCNA is controlled by DNA. *EMBO J.*, **27**, 2422–2431.

43. Burkovics,P., Sebesta,M., Sisakova,A., Plault,N., Szukacsov,V., Robert,T., Pinter,L., Marini,V., Kolesar,P., Haracska,L. *et al.* (2013) Srs2 mediates PCNA-SUMO-dependent inhibition of DNA repair synthesis. *EMBO J.*, **32**, 742–755.

44. Li,X., Stith,C.M., Burgers,P.M. and Heyer,W.D. (2009) PCNA is required for initiation of recombination-associated DNA synthesis by DNA polymerase delta. *Mol. Cell*, **36**, 704–713.

45. Wilson,M.A., Kwon,Y., Xu,Y., Chung,W.H., Chi,P., Niu,H., Mayle,R., Chen,X., Malkova,A., Sung,P. *et al.* (2013) Pif1 helicase and Poldelta promote recombination-coupled DNA synthesis via bubble migration. *Nature*, **502**, 393–396.

46. Armstrong,A.A., Mohideen,F. and Lima,C.D. (2012) Recognition of SUMO-modified PCNA requires tandem receptor motifs in Srs2. *Nature*, **483**, 59–63.

47. Ikenaga,M., Ichikawa-Ryo,H. and Kondo,S. (1975) The major cause of inactivation and mutation by 4-nitroquinoline 1-oixde in Escherichia coli: excisable 4NQO-purine adducts. *J. Mol. Biol.*, **92**, 341–356.

48. Spence,J., Sadis,S., Haas,A.L. and Finley,D. (1995) A ubiquitin mutant with specific defects in DNA repair and multiubiquitination. *Mol. Cell. Biol.*, **15**, 1265–1273.

49. Ulrich,H.D. and Jentsch,S. (2000) Two RING finger proteins mediate cooperation between ubiquitin-conjugating enzymes in DNA repair. *EMBO J.*, **19**, 3388–3397.

50. Parker,J.L. and Ulrich,H.D. (2012) A SUMO-interacting motif activates budding yeast ubiquitin ligase Rad18 towards SUMO-modified PCNA. *Nucleic Acids Res.*, **40**, 11380–11388.

51. Unk,I., Hajdu,I., Blastyak,A. and Haracska,L. (2010) Role of yeast Rad5 and its human orthologs, HLTF and SHPRH in DNA damage tolerance. *DNA Repair (Amst.)*, **9**, 257–267.

52. Shkedy,D., Singh,N., Shemesh,K., Amir,A., Geiger,T., Liefshitz,B., Harari,Y. and Kupiec,M. (2015) Regulation of Elg1 activity by phosphorylation. *Cell Cycle*, 0.

53. Tong,K. and Skibbens,R.V. (2015) Pds5 regulators segregate cohesion and condensation pathways in Saccharomyces cerevisiae. *Proc. Natl. Acad. Sci. U.S.A.*, **112**, 7021–7026.

54. Hishida,T., Hirade,Y., Haruta,N., Kubota,Y. and Iwasaki,H. (2010) Srs2 plays a critical role in reversible G2 arrest upon chronic and low doses of UV irradiation via two distinct homologous recombination-dependent mechanisms in postreplication repair-deficient cells. *Mol. Cell. Biol.*, **30**, 4840–4850.

55. Boehm,E.M. and Washington,M.T. (2016) R.I.P. to the PIP: PCNA-binding motif no longer considered specific: PIP motifs and other related sequences are not distinct entities and can bind multiple proteins involved in genome maintenance. *BioEssays*.

56. Lee,K.Y. and Myung,K. (2008) PCNA modifications for regulation of post-replication repair pathways. *Mol. Cells*, **26**, 5–11.

57. Liefshitz,B., Steinlauf,R., Friedl,A., Eckardt-Schupp,F. and Kupiec,M. (1998) Genetic interactions between mutants of the 'error-prone' repair group of Saccharomyces cerevisiae and their effect on recombination and mutagenesis. *Mut. Res.*, **407**, 135–145.